To cite this article: SU L, WANG X H, XIAO J M. Ship micro-grid reconfiguration based on multiobjective optimization algorithm [J/OL]. Chinese Journal of Ship Research, 2020, 15(3). http://www.ship-research.com/EN/Y2020/V15/I3/169.

DOI: 10.19693/j.issn.1673-3185.01534

Ship micro-grid reconfiguration based on multiobjective optimization algorithm

SU Li, *WANG Xihuai**, *XIAO Jianmei*

Logistics Engineering College, Shanghai Maritime University, Shanghai 201306, China

Abstract: [**Objectives**] In order to solve the problem of poor convergence and distribution of the existing constrained multiobjective optimization algorithms in solving the ship micro-grid reconfiguration, a constrained multiobjective optimization method based on two-stage differential evolution (TSDE) algorithm is proposed. [**Methods**] Firstly, in the first stage, the two-population hybrid method (i.e. self-adaptive penalty function method and feasibility rule) was used to deal with the constraints. Secondly, in the second stage, the two populations generated in the first stage were merged into a single population, and the feasibility rule was adopted to solve the constrained optimization problem. Finally, different elitist selection strategies and improved non-parametric mutation operators were adopted in different stages to further optimize the differential evolution algorithm. [**Results**] The simulation results show that the minimum load loss obtained by TSDE algorithm under the fault 1 and the fault 2 is 185 and 940 A lower than that of chaotic migration and parameterless mutation differential evolution (CMPMDE) and environment pareto dominated selection differential evolution (EPDSDE), respectively. The minimum switching operands obtained by the TSDE algorithm are 1 time more than that of CMPMDE algorithm under the fault 1, and are the same as that of EPDSDE algorithm. Under the fault 2, the minimum switching operands of the proposed algorithm are 1 time less than those of CMPMDE algorithm and EPDSDE algorithm. [**Conclusions**] The set of optimal non-inferior solutions obtained by TSDE algorithm is closer to the real Pareto frontier and distributes more evenly, so the method can ensure that the ship is operated safely and steadily when the reconfiguration time is satisfied.

Key words: micro-grid reconfiguration; multiobjective optimization; two-stage differential evolution algorithm; elitist selection strategies; improved non-parametric mutation operator

CLC number: U665.12

0 Introduction

With the development trend of large-scale and automated ships, the capacity of the power system is also increasing. In the case of a power system fault, algorithms including particle swarm optimization [1-5], genetic algorithm [6-9], clonal algorithm [10], and differential evolution algorithm [11-12] can be used to reconfigure the ship micro-grid fault, so as to quickly restore the normal power supply of important loads. However, there are few research achievements in the reconfiguration of ship micro-grid by using the constrained multiobjective optimization algorithm, mainly because of the disadvantages of the multiobjective optimization algorithm, such as parallel optimization of multiple problems, large computation, and difficult operation. Therefore, it is one of the difficulties that need to be broken through to seek an algorithm [13] that can satisfy constraints and make the Pareto solution set converge to the optimal non-dominated frontier and have a uniform distribution.

In recent years, scholars have tried to adopt a multiobjective optimization algorithm to solve the problem of ship micro-grid reconfiguration. Based on the

Received: 2019-02-27 **Accepted:** 2019-04-21

Supported by: National Natural Science Foundation of China (61573240)

Authors: SU Li, female, born in 1993, master degree candidate. Research interest: complex system control and optimization. E-mail: 937453863@qq.com

WANG Xihuai, male, born in 1961, Ph.D., professor. Research interest: complex system modeling and control, system optimization and simulation, and transport control engineering. E-mail: wxh@shmtu.edu.cn

XIAO Jianmei, female, born in 1962, master, professor. Research interest: intelligent control, rough set theory, and logistics system optimization. E-mail: jmxiao@shmtu.edu.cn

***Corresponding author:** WANG Xihuai

traditional non-dominated sorting genetic algorithm (NSGA), Zhang [9] proposed an NSGA-II algorithm that considers the elitist selection strategy and congestion. Although its convergence had been improved and the convergence time had been greatly shortened, it did not fully consider constraints. Ma et al. [14] proposed a differential evolution algorithm based on chaotic migration and non-parametric mutation. This algorithm had a simple structure and effectively avoided premature phenomenon, but it eliminated excellent infeasible solutions, resulting in poor convergence and distribution in the search for optimal non-inferior solutions. By improving the selection strategy in Reference [14], Ma et al. [15] saved the excellent information of the infeasible solutions, thus improving the convergence, but the problems of poor distribution and slow convergence remained to be solved.

Based on the above information, before the reconfiguration of the micro-grid, this paper will determine the power supply path of partial loads and calculate the total power of the branch loads through the correlation matrix method of load branches [4], which can not only reduce the amount of data analysis but also lay a foundation for the establishment of constraints. This paper proposes a two-stage differential evolution (TSDE) algorithm because the advantages and disadvantages of constrained multiobjective optimization algorithm are greatly related to the processing of constraints and the selection of evolution algorithm [13]: In the first stage, the two-population hybrid method is adopted to deal with the constrained optimization problem, and in the second stage, the improved feasibility rule is adopted to solve the constrained problem. The Tent map chaotic sequence, the improved non-parametric mutation operator, and the elitist selection strategy are also used to optimize the differential evolution algorithm. Finally, in order to verify the feasibility and effectiveness of the TSDE algorithm, we compare the results of the algorithm with the simulation results of the algorithm based on chaotic migration and parameterless mutation differential evolution (CMPMDE) [14] and the algorithm based on environment Pareto dominated selection differential evolution (EPDSDE) [15] to provide a reference for the reconfiguration design of ship micro-grid faults.

1 Mathematical model of ship mic-rogrid reconfiguration

Fig. 1 shows the structure of the annular power supply system of the ship, with a generator capacity of 320 kW, bus capacity of 710 A, and branch capacity of 420 A. The operating current and load grade of 20 loads are shown in Table 1 [15]. In Fig. 1, the impor-

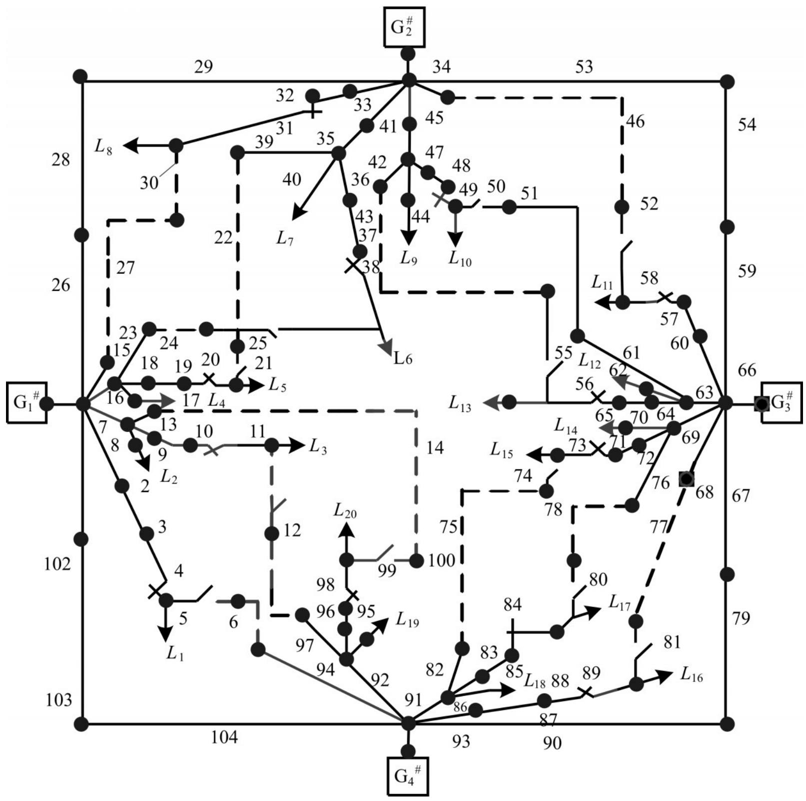

Fig.1 Schematic diagram of power supply system

tant load is provided with two supply paths by automatic bus transfer (ABT), in which the solid line and the dotted line respectively represent the power supply with a normal path and the power supply with an alternative path. The symbol " × " is ABT switch which is always off; "—⁄—" is ABT switch which is always on; " ↓ " is the load L_1–L_{20}; " • " is the endpoint of a device or line; the numbers 1–104 are lines B_1–B_{104} and $G_1^\#$–$G_4^\#$ are generators.

Table 1 Operating current and load grade of system load

Load number	Operating current /A	Load grade	Load number	Operating current /A	Load grade
L_1	70	Grade 1	L_{11}	225	Grade 1
L_2	120	Grade 3	L_{12}	205	Grade 3
L_3	200	Grade 2	L_{13}	110	Grade 2
L_4	150	Grade 3	L_{14}	72	Grade 3
L_5	160	Grade 2	L_{15}	87	Grade 2
L_6	100	Grade 1	L_{16}	100	Grade 1
L_7	80	Grade 3	L_{17}	205	Grade 2
L_8	325	Grade 1	L_{18}	200	Grade 3
L_9	185	Grade 3	L_{19}	165	Grade 3
L_{10}	44	Grade 2	L_{20}	30	Grade 2

1.1 Objective function

Ship micro-grid reconfiguration is a discrete combinatorial optimization problem with multi-constraint and multiobjective [9]. According to the characteristics of the ship power system, the requirements of minimum load loss and minimum switching operands should be satisfied on the premise of meeting the constraints of network topology, generator capacity, load priority, branch capacity, etc., so as to ensure the rapidity and safety of power system reconfiguration and recovery.

1.1.1 Minimum load loss

According to the requirements of load priority, this paper divides the load into three grades (Table 1): The first grade is important load; the second grade is secondary important load, and the third grade is non-important load. Under any working condition, the first-grade load should be restored first, then the second-grade load, and finally the third-grade load. In the process of micro-grid reconfiguration, attention should be paid to reducing load loss to ensure the normal operation of the power system of the ship, and the objective function $\min f_1$ is

$$\min f_1 = a_1\sum_{t=1}^{k_1}\left(1-X_{1t}\right)L_{\mathrm{g}1t} + a_2\sum_{h=1}^{k_2}\left(1-X_{2h}\right)L_{\mathrm{g}2h} + a_3\sum_{w=1}^{k_3}\left(1-X_{3w}\right)L_{\mathrm{g}3w} \quad (1)$$

where L_{g1t}, L_{g2h}, L_{g3w} are the load capacity of the first, second, and third grades respectively, and their values are shown in Table 1; X_{1t}, X_{2h}, X_{3w} are 1 or 0, respectively representing the power supply and unloading operations of the corresponding load; t, h, w are the number of first-grade, second-grade and third-grade loads respectively, and the maximum values of k_1, k_2, k_3 are 5, 7, 8 respectively; $a_1 = L_{\max 2}L_{\max 3}/L_{\min 1}L_{\min 2}$ = 20, $a_2 = L_{\max 3}/L_{\min 2} = 7$, $a_3 = 1$, where $L_{\max2}$ and $L_{\max3}$ are the maximum values of second-grade load and third-grade loads, and $L_{\min1}$ and $L_{\min2}$ are the minimum values of first-grade load and second-grade load, the values are shown in Table 1.

1.1.2 Minimum switching operands

The switching operands will directly affect the recovery time of the power system: The larger operand number means the slower recovery and vice versa. Its objective function $\min f_2$ is

$$\min f_2 = \sum_{e=1}^{h_1}(1-H_e) + \sum_{r=1}^{h_2} Z_{\mathrm{A}r} \quad (2)$$

where e and r are respectively the number of power supply branch switches under the third-grade and first-grade or second-grade loads, the maximum values are h_1 and h_2 respectively; H_e is 1 or 0, respectively indicating that switch e maintains the original off state or changes from off state to on state in reconfiguration; $Z_{\mathrm{A}r}$ is 1 or 0, respectively indicating that switch r changes from normal-path power supply to the alternative-path power supply or maintains the original normal path power supply [14].

1.2 Constraint condition

1.2.1 Radial topology constraints of power systems

For first-grade and second-grade loads, they can only be powered by one of the normal or alternative paths during reconfiguration.

$$\sum_{k\in\Omega_i}\left(1-z_k\right) = \sum_{l\in\Omega_i} z_l \quad (3)$$

where Ω_i is a set of automatic transfer switches consisting of normal switch k and alternative switch l of first-grade and second-grade loads; z_k and z_l are the normal switch and alternative switch of the same load, whose on and off states are 0 and 1.

1.2.2 Capacity constraint

During the reconfiguration, it should be noted that branch capacity and generator capacity should not be overloaded. If they are overloaded, unloading should be considered.

$$\sum_{a=1}^{m_1} X_{ab} s_a \leqslant M_b \tag{4}$$

where a = 1, 2, ⋯, m_1, is the number of loads a or branches a, where m_1 is the maximum value of a; X_{ab} is 0 or 1, indicating that the connection switch state of load a and branch b (or branch a and distribution board b) is on or off; s_a is the power consumption of load or branch, A; M_b is the capacity margin of branch b, A.

1.3 Constrained optimization problem

1.3.1 Constrained multiobjective processing of the first stage

First, through Eq. (5) and Eq. (6), the original constrained problems of the first population and the second population are transformed into unconstrained problems and constrained problems with two objectives respectively. Then, the corresponding differential evolution algorithm is used for simultaneous optimization, as detailed in section 3.

1) In the first population, the constrained multiobjective optimization problem is transformed into the unconstrained multiobjective optimization problem by using the adaptive penalty function method, namely

$$\begin{cases} \min \Omega_1(\boldsymbol{X}) = f_1(\boldsymbol{X}) + \alpha_{12} f_3(\boldsymbol{X}) \\ \min \Omega_2(\boldsymbol{X}) = f_2(\boldsymbol{X}) + \alpha_{12} f_3(\boldsymbol{X}) \\ f_3(\boldsymbol{X}) = \sum_{b=1}^{o} \max\{0, g_b(\boldsymbol{X})\} \\ g_b(\boldsymbol{X}) = \sum_{a=1}^{m_1} X_{ab} s_a - M_b \leqslant 0, \quad b = 1, 2, \cdots, o \end{cases} \tag{5}$$

where $f_1(\boldsymbol{X})$, $f_2(\boldsymbol{X})$, $f_3(\boldsymbol{X})$ are original objective function 1, original objective function 2, and constraint violation function respectively, where $\boldsymbol{X}$ is a discrete decision vector; $\Omega_1(\boldsymbol{X})$ and $\Omega_2(\boldsymbol{X})$ are converted objective function 1 and objective function 2 respectively; $g_b(\boldsymbol{X})$ is the constraint condition b which includes branch capacity no-overloading and generator capacity misloading, where b = 1, 2, ⋯, o, and o is the maximum value of b.

Here

$$\alpha_{12} = \begin{cases} 1 + 2\sqrt{1-2\rho}, & 0 \leqslant \rho \leqslant 0.5 \\ 1, & 0.5 < \rho \leqslant 1 \end{cases}$$

where ρ is the ratio of feasible solution.

2) In the second population, the constrained multiobjective function is as follows:

$$\begin{cases} \min \left(f_1(\boldsymbol{X}), f_2(\boldsymbol{X}) \right) \\ g_b(\boldsymbol{X}) = \sum_{a=1}^{m_1} X_{ab} s_a - M_b \leqslant 0, \quad b = 1, 2, \cdots, o \end{cases} \tag{6}$$

1.3.2 Constrained multiobjective processing of the second stage

First of all, in order to accelerate the convergence, we only adopt the single population feasibility rule (Eq. (6)) in the second stage to transform the original constrained problem into the constrained problem with two objectives, so as to reduce the calculation amount. Then, the differential evolution algorithm in the second stage is adopted, as detailed in section 3.

During the constrained multiobjective processing in the second stage, the following definitions are made:

1) Definition 1 (Pareto dominance): When $\boldsymbol{X}^*$ is the feasible solution set of the discrete decision vector, for any two discrete decision vectors $\boldsymbol{X}_m$ and $\boldsymbol{X}_n \in \boldsymbol{X}^*$, if and only if $f_1(\boldsymbol{X}_m) < f_1(\boldsymbol{X}_n) \wedge f_2(\boldsymbol{X}_m) \leqslant f_2(\boldsymbol{X}_n)$ or $f_1(\boldsymbol{X}_m) \leqslant f_1(\boldsymbol{X}_n) \wedge f_2(\boldsymbol{X}_m) < f_2(\boldsymbol{X}_n)$, then the vector $\boldsymbol{X}_m$ Pareto-dominates vector $\boldsymbol{X}_n$, namely, $\boldsymbol{X}_n \prec \boldsymbol{X}_m$.

2) Definition 2 (Pareto optimal solution): If and only if $\neg \exists \boldsymbol{X}_n \in \boldsymbol{X}^*$ and $\boldsymbol{X}_m \prec \boldsymbol{X}_n$, then vector $\boldsymbol{X}_m \in \boldsymbol{X}^*$ is regarded as Pareto optimal solution (Pareto non-inferior solution) of the two objectives (Eq. (5) and Eq. (6)), where $\boldsymbol{X}_n$ is any solution vector in the feasible region.

3) Definition 3 (Pareto optimal solution set): The Pareto optimal solution set of the two-objective problem (Eq. (5) and Eq.(6)) is denoted as $\boldsymbol{PS}$, and then $\boldsymbol{PS} = \{\boldsymbol{X}_m \in \boldsymbol{X}^* \mid \neg \exists \boldsymbol{X}_n \in \boldsymbol{X}^*, \boldsymbol{X}_m \prec \boldsymbol{X}_n\}$.

4) Definition 4 (Pareto frontier). For the two-objective optimization problem (Eq. (5) and Eq.(6)), the image set of the Pareto optimal solution set in the target space is Pareto frontier (denoted as $\boldsymbol{PF}$), and then $\boldsymbol{PF} = \{f(\boldsymbol{X}_u) = (f_1(\boldsymbol{X}_u), f_2(\boldsymbol{X}_u)) \mid \boldsymbol{X}_u \in \boldsymbol{PS}\}$, where $\boldsymbol{X}_u$ is the optimal non-inferior solution.

2 Two-stage differential evolution algorithm

2.1 Population initialization

Using Tent map chaotic sequence to initialize the population can not only avoid the inhomogeneity of initializing individuals but also solve the problem of search time and space. Its mathematical expression is as follows:

$$\begin{cases} r_{1,j} = rand(1) \\ r_{i+1,j} = \begin{cases} 2r_{i,j}, & 0 \leqslant r_{i,j} \leqslant 0.5 \\ 2\left(1 - r_{i,j}\right), & 0.5 < r_{i,j} \leqslant 1 \end{cases} \end{cases} \tag{7}$$

where $r_{i,j}$ and $rand(1)$ are both random numbers in the interval [0, 1], where i = 1, 2, ..., N −1 and j=1, 2, ⋯, d (N−1 and d are the maximum values of i and j respectively).

The upper boundary constraint $x_{j\max}$ and the lower boundary constraint $x_{j\min}$ of the continuous decision variable are defined, and $r_{i,j}$ are mapped to the search space ($x_{j\min}$, $x_{j\max}$). There is

$$x_{i,j} = x_{j\min} + \left(x_{j\max} - x_{j\min}\right) r_{i,j} \tag{8}$$

where $x_{i,j}$ is the j-th continuous decision variable of the ith individual.

2.2 Discretization method

The reconfiguration of ship micro-grid is a discrete problem, but the initialized individual $x_{i,j}$ is a continuous individual, so the continuous individual needs to be discretized in this paper [9], specifically as follows:

For the first-grade load and the second-grade load, there is

$$X_{i,j} = \begin{cases} 0, & \text{if } x_{i,j} \in [0, 0.5) \\ 1, & \text{else if } x_{i,j} \in [0.5, 1.5] \\ 2, & \text{else if } x_{i,j} \in (1.5, 2] \end{cases} \tag{9}$$

For the third-grade load, there is

$$X_{i,j} = \begin{cases} 0, & \text{if } x_{i,j} \in [0, 0.25) \\ 1, & \text{else if } x_{i,j} \in [0.25, 1] \end{cases} \tag{10}$$

where $X_{i,j}$ is the decision variable after discretization, in which 0 represents load loss, 1 represents normal-path power supply, and 2 represents alternative-path power supply.

2.3 Improved mutation strategy and adaptive crossover operation

For the discrete decision variables, if the traditional differential evolution algorithm is used for crossover and mutation processing, the generated decision variables cannot satisfy the three discrete states of 0, 1, 2. Therefore, an improved non-parametric mutation strategy will be designed in this paper.

2.3.1 Mutation operation

1) 0 and 1 states of power supply without an alternative path [15]:

$$\boldsymbol{V}_{i,j}^{G+1} = \boldsymbol{X}_{r1,j}^{G} + (-1)^{\boldsymbol{X}_{r1,j}^{G}} \left| \boldsymbol{X}_{r2,j}^{G} - \boldsymbol{X}_{r3,j}^{G} \right| \tag{11}$$

where $\boldsymbol{V}_{i,j}^{G+1}$ is the discrete mutation individual and G is the number of iterations; $\boldsymbol{X}_{r1,j}^{G}$, $\boldsymbol{X}_{r2,j}^{G}$, $\boldsymbol{X}_{r3,j}^{G}$ are discrete individuals randomly selected from the entire parent population. When $\left|\boldsymbol{X}_{r2,j}^{G} - \boldsymbol{X}_{r3,j}^{G}\right|$ =1, vector $\boldsymbol{X}_{r1,j}^{G}$ will directly mutate from 0 to 1 or from 1 to 0; when $\left|\boldsymbol{X}_{r2,j}^{G} - \boldsymbol{X}_{r3,j}^{G}\right|$=0, $\boldsymbol{X}_{r1,j}^{G}$ stays the same.

2) 0, 1, 2 states of power supply with an alternative path:

$$\boldsymbol{V}_{i,j}^{G+1} = \begin{cases} \left| \boldsymbol{X}_{r1,j}^{G} + (-1)^{\boldsymbol{X}_{r1,j}^{G}} \left| \boldsymbol{X}_{r2,j}^{G} - \boldsymbol{X}_{r3,j}^{G} \right| \right|, & \text{if } \boldsymbol{X}_{r1,j}^{G} = 0 \\ \left| \boldsymbol{X}_{r1,j}^{G} + (-1) \left| \boldsymbol{X}_{r2,j}^{G} - \boldsymbol{X}_{r3,j}^{G} \right| \right|, & \text{if } \boldsymbol{X}_{r1,j}^{G} = 1 \text{ or } \boldsymbol{X}_{r1,j}^{G} = 2 \end{cases} \tag{12}$$

When $\left|\boldsymbol{X}_{r2,j}^{G} - \boldsymbol{X}_{r3,j}^{G}\right| \neq 0$, vector $\boldsymbol{X}_{r1,j}^{G}$ may mutate or remain unchanged; when $\left|\boldsymbol{X}_{r2,j}^{G} - \boldsymbol{X}_{r3,j}^{G}\right|$=0, $\boldsymbol{X}_{r1,j}^{G}$ remains the same.

2.3.2 Crossover operation

$$\begin{cases} CR = CR_0 \mathrm{e}^{-2\left(\frac{G}{G_{\max}}\right)} \\ \boldsymbol{U}_j^{G+1} = \begin{cases} \boldsymbol{V}_j^{G+1}, & \text{rand}(1) < CR \mid j = r_0 \\ \boldsymbol{X}_j^{G}, & \text{else} \end{cases} \end{cases} \tag{13}$$

where CR is an adaptive crossover operator; CR_0 is the initial value of crossover operator; $G_{\max}$ is the maximum number of iterations; $\boldsymbol{U}_j^{G+1}$ is the discrete experimental vector of the jth decision variable of G + 1 iterations; $\boldsymbol{V}_j^{G+1}$ is the discrete mutation vector of the j-th decision variable of G+1 iterations. $\boldsymbol{X}_j^{G+1}$ is the discrete objective vector of the jth decision variable of G iterations; r_0 is a randomly selected sequence of values in the interval [1, 2, ⋯, d].

2.4 Improved elitist selection strategy

2.4.1 The first stage

1) The selection strategy of the first population: first, the parent population and the offspring population are combined into one population, and the population individuals are subjected to fast non-dominated sorting and congestion calculation [9]. Then, the individual grade is taken as the function value of fitness and congestion to make comparison and selection. Finally, N^* excellent individuals are selected. The specific steps are as follows:

(1) $\boldsymbol{P}^G_1$, the generation-G parent population of the first population, and $\boldsymbol{Q}^G_1$, the generation-G descendant population, are combined into a generation-G total population $\boldsymbol{R}^G_1$.

(2) The total population $\boldsymbol{R}^G_1$ is subject to fast non-dominated sorting, generating k non-dominated sets [$\boldsymbol{F}_1, \boldsymbol{F}_2, \cdots, \boldsymbol{F}_K$], and then the congestion is calculated. Since the non-dominated set $\boldsymbol{F}_1$ has the highest grade of individuals, it is the optimal individual

in the total population $\boldsymbol{R}^{G}_{1}$, while the grade of $\boldsymbol{F}_2$, $\boldsymbol{F}_3, \cdots, \boldsymbol{F}_K$ is reduced in turn. The procedures of fast non-dominated sorting and congestion sorting and the calculation equation of congestion refer to Reference [9].

(3) According to the descending order of [$\boldsymbol{F}_1$, $\boldsymbol{F}_2$, $\cdots$, $\boldsymbol{F}_K$], they are added to $\boldsymbol{P}^{G+1}_{1}$, the generation-(G + 1) parent population, until the number of individuals in $\boldsymbol{P}^{G+1}_{1}$ is greater than N^*. At this time, $\boldsymbol{F}_{K1}$ is just added.

(4) As the number of individuals in $\boldsymbol{F}_{K1}$ exceeds the target value, the congestion of all individuals in $\boldsymbol{F}_{K1}$ is sorted. Then the individuals $N^*-n_1-n_2-\cdots-n_{K1-1}$ are added to $\boldsymbol{P}^{G+1}_{1}$ respectively, and the number of individuals in $\boldsymbol{P}^{G+1}_{1}$ is exactly N^*, where $n_1, n_2, \cdots, n_{K1-1}$ are the individual numbers of non-dominated sets $\boldsymbol{F}_1, \boldsymbol{F}_2, \cdots, \boldsymbol{F}_{K1-1}$.

2) The selection strategy of the second population: an environment Pareto dominated selection strategy is adopted [16]. Through fast non-dominated sorting of the population individuals, and calculating the degree of violation constraint $C(i)$, congestion $W(i)$ and boundary distance $D(i)$, we select N^*excellent individuals. First, the generation-G parent population $\boldsymbol{P}^{G}_{2}$ and the generation-G descendant population $\boldsymbol{Q}^{G}_{2}$ merge into a generation-G total population $\boldsymbol{R}^{G}_{2}$. Then, through the tournament selection method, two individuals are randomly selected and the better individual is selected and saved to the generation-(G + 1) $\boldsymbol{P}^{G+1}_{2}$ until N^*excellent individuals are selected. The comparison and selection strategies of the two individuals are as follows:

(1) If both of them are feasible solutions, the non-dominated one is selected. If the two individuals do not control each other, the one with greater congestion is selected.

(2) If an individual is a feasible solution and the other individual is an infeasible solution, and the boundary distance of the feasible solution is less than the infeasible solution, then the feasible solution individual is selected; otherwise, the non-dominated one is selected. If the two individuals do not control each other, the one with greater congestion is selected.

(3) If both of the two individuals are infeasible solutions, the non-dominated individual is selected. If the two individuals do not control each other, the individual with lower violation constraint is selected.

The formulas of constraint violation degree $C(i)$, boundary distance $D(i)$, and congestion $W(i)$ are as follows:

$$C(i)=\sum_{b=1}^{o}\max\left(0, g_b\left(\boldsymbol{X}_i\right)\right) \tag{14}$$

$$D(i)=\sum_{b=1}^{o}\left|g_b\left(\boldsymbol{X}_i\right)\right| \tag{15}$$

$$W(i)=\begin{cases}\infty, i \text{ is in the boundary}\\ \sum_{q=1}^{k_4}\left|\dfrac{f_q(i+1)-f_q(i-1)}{f_q(N)-f_q(1)}\right|, \text{ else}\end{cases} \tag{16}$$

where $g_b(\boldsymbol{X}_i)$ is the function value of the ith individual under the inequality constraint b; q=1, 2, $\cdots$, k_4 is the number of objective functions, where k_4 is the maximum value of q; N is the population number; $f_q(1)$, $f_q(2)$, $\cdots$, and $f_q(N)$ is the ascending order of all individuals in the objective function q.

2.4.2 The second stage

1) Firstly, $\boldsymbol{P}^{S+1}$ of the generation-(S + 1) parent population and $\boldsymbol{Q}^{S+1}$ of the generation-(S + 1) descendant population are combined to form a generation-(S + 1) total population $\boldsymbol{R}^{S+1}$. Then, the total population $\boldsymbol{R}^{S+1}$ is divided into a feasible solution set $\boldsymbol{Z}_1$ and an infeasible solution set $\boldsymbol{Z}_2$ by constraint conditions.

2) According to the selection strategy in Reference [15], the capacities N_1 and N_2 of the feasible solution set and infeasible solution set are set respectively.

3 The concrete steps of algorithm implementation

1) Coding. 0, 1, 2 and 0, 1 are coded for important and non-important loads respectively, where 0 represents load loss, 1 represents normal-path power supply and 2 represents alternative-path power supply.

2) Initialization. We set the population number N, the capacities N_1 and N_2 of feasible and infeasible solution sets, the balance coefficient λ, and the maximum number of iterations $G_{\max}$.

3) If $G \leqslant$ S, go to step 4); otherwise, go to step 5).

4) The first stage. First of all, the Eq. (7) and Eq. (8) are used to generate initialized $\boldsymbol{P}_1$ of the first population and $\boldsymbol{P}_2$ of the second population, and discrete operation of individuals in $\boldsymbol{P}_1$ and $\boldsymbol{P}_2$ is carried out by Eq. (9) and Eq. (10). In addition, the objective function value of the first population and the objective function value and constraint degree of the second population are respectively calculated by Eq. (1), Eq. (2), Eq. (4), Eq. (5), and Eq. (6). Then, the parent-generation individuals in $\boldsymbol{P}_1$ and $\boldsymbol{P}_2$ are subject to mutation and crossover operations respectively to produce the offspring populations $\boldsymbol{Q}_1$ and $\boldsymbol{Q}_2$. Finally, according to the selection strategy in section 2.4.1,

N^* excellent individuals of $\boldsymbol{P}_1$ and $\boldsymbol{P}_2$ are selected respectively.

5) The second stage. First, the first population and the second population after the evolution of stage 1 merge into one population, which is regarded as the parent population $\boldsymbol{P}$ of stage 2, and the objective function value and constraint degree of the parent population are calculated according to Eq. (1), Eq. (2), Eq. (4) and Eq. (6). Then, the parent population $\boldsymbol{P}$ is subject to mutation and crossover to produce the descendant population $\boldsymbol{Q}$. Finally, according to the selection strategy in section 2.4.2, the excellent feasible solution set $\boldsymbol{Z}_1$ and infeasible solution set $\boldsymbol{Z}_2$ are selected.

6) The termination condition is judged. If $G<G_{\max}$, return to step 3), otherwise, the algorithm is terminated and the feasible solution set is output.

4 Experimental simulation analysis

In this paper, the topology structure of the annular ship grid is adopted as the simulation model (Fig. 1), and its load attributes are shown in Table 1. In order to compare the TSDE algorithm proposed in this paper with the CMPMDE algorithm [14] and EPDSDE algorithm [15], we set the same parameters and faults in the simulation link, as follows:

1) Parameter settings. The initialized switch state is set to load code value of 1. The size of the first population and the second population is set as N=50, the feasible solution set and the infeasible solution set as N_1= 50 and N_2= 25, the balance coefficient as λ = 0.2, the initial crossover factor value as CR_0=0.85, and the maximum number of iterations as $G_{\max}$=50. The value of S can be determined according to the actual fault situation.

2) Fault 1. It is assumed that branches B_{10} and B_{63} are damaged, resulting in the unloading of load L_{12}, damage of normal power supply path of load L_3 and L_{13}, and damage of alternative path of load L_{10}.

3) Fault 2. It is assumed that No. 1 generator $G_1^{\#}$ stops power supply due to fault, resulting in the unloading of load L_2 and L_4, damage of normal power supply path of load L_1, L_3, and L_5, and damage of alternative paths of load L_6, L_8 and L_{20}.

Three algorithms will be run independently 50 times, and an operation result will be randomly selected. In order to reduce human choice time, improve the efficiency of micro-grid reconfiguration, this paper chooses an optimal nondominant solution in multiple solutions of the TSDE algorithm, with minimum load loss as the main consideration factor. The simulated comparison results of the three algorithms under fault 1 and fault 2 are shown in Table 2 and Table 3 respectively.

Table 2 Comparison of different methods for reconfiguration results under fault 1

Algorithm	Optimal nondominant solution	Minimum load loss/A	Minimum switching operands/times
CMPMDE	11211111011021112111	390	5
EPDSDE	11211211011021112111	390	6
TSDE	11212112111021112111	205	6

Table 3 Comparison of different methods for reconfiguration results under fault 2

Algorithm	Optimal nondominant solution	Minimum load loss/A	Minimum switching operands/times
CMPMDE	20200111121011121101	1 760	9
EPDSDE	20200111121011121101	1 760	9
TSDE	20202111011111111001	820	8

Table 2 and Table 3 show that under fault 1, the minimum load loss of optimal non-inferior solution obtained by TSDE algorithm is 185 A lower than that of CMPMDE algorithm and EPDSDE algorithm, and its minimum switching operands are one time more than those of CMPMDE algorithm, and the same as those of EPDSDE algorithm. Under fault 2, the minimum load loss of the TSDE algorithm is 940 A smaller than that of CMPMDE algorithm and EPDSDE algorithm, and its minimum switching operands are one time smaller than those of CMPMDE algorithm and EPDSDE algorithm. According to the definition of Pareto dominance and Pareto optimal solution, it can be seen that under fault 1, the optimal non-inferior solution of TSDE algorithm and CMPMDE algorithm does not dominate each other, but the optimal non-inferior solution obtained by TSDE algorithm dominates EPDSDE algorithm, namely that the optimal non-inferior solution of TSDE algorithm is superior to EPDSDE algorithm. Under fault 2, the optimal non-inferior solution obtained by the TSDE algorithm can dominate the CMPMDE algorithm and EPDSDE algorithm, namely that the optimal non-inferior solution of the TSDE algorithm is superior to that of the CMPMDE algorithm and EPDSDE algorithm. In summary, the TSDE algorithm has significantly better convergence than the CMPMDE algorithm and EPDSDE algorithm.

In the case of ship fault, the fault-free load should be restored immediately under the premise of satisfying the constraints, so reconfiguration time is a very important performance index. After running the TSDE algorithm independently 50 times, we count the optimal convergence algebra GEN_{best}, average convergence algebra GEN_{avr}, optimal convergence time T_{best}, and average convergence time T_{avr} and compare them with the recorded data in References [14] and [15]. The results are shown in Table 4 and Table 5. Since there is no running time data of CMPMDE algorithm and EPDSDE algorithm in References [14] and [15], the corresponding positions in Table 4 and Table 5 are blank.

Table 4 Comparison of different methods for reconfiguration time under fault 1

Algorithm	GEN_{best}/times	GEN_{avr}/times	T_{best}/s	T_{avr}/s
CMPMDE	4	5.8		
EPDSDE	4	5.8		
TSDE	23	23.6	6.995	7.018

Table 5 Comparison of different methods for reconfiguration times under fault 2

Algorithm	GEN_{best}/times	GEN_{avr}/times	T_{best}/s	T_{avr}/s
CMPMDE	4	4.8		
EPDSDE	5	5.3		
TSDE	29	29.8	7.528	7.728

It can be seen from Table 4 that under fault 1, the optimal iteration times of TSDE algorithm converging to the optimal non-inferior solution set are 19 times larger than those of CMPMDE algorithm and EPDSDE algorithm, and the average iteration times are 17.8 times larger. It can be seen from Table 5 that under fault 2, the optimal iteration times of the TSDE algorithm converging to the optimal non-inferior solution set are 25 and 24 times larger than those of the CMPMDE algorithm and EPDSDE algorithm, and the average iteration times are 25 and 24.5 times larger, respectively. It can be seen that the optimal and average iteration times in Table 4 and Table 5 are both greater than those of the CMPMDE algorithm and EPDSDE algorithm. This is because, in the first stage, the paper uses the two-population hybrid method (i.e., the adaptive penalty function method and feasibility rule) to deal with the constrained optimization problem. In addition, an improved selection strategy for the feasible and infeasible solutions is adopted. Therefore, it increases the diversity of the populations and expands the population size, which leads to relatively slow convergence. However, according to the simulation results in Table 4 and Table 5, both the optimal convergence time and the average convergence time of the TSDE algorithm are controlled within 10 s, which can meet the reconfiguration time requirements of the ship micro-grid.

In order to compare the uniformity and approximation of the Pareto optimal solution set of the three algorithms, we make the three algorithms run independently 50 times, and the results of one run are randomly selected, as shown in Fig. 2 and Fig. 3. According to the simulation results, the Pareto frontier of the TSDE algorithm is superior to the CMPMDE algorithm and EPDSDE algorithm in uniformity and approximation.

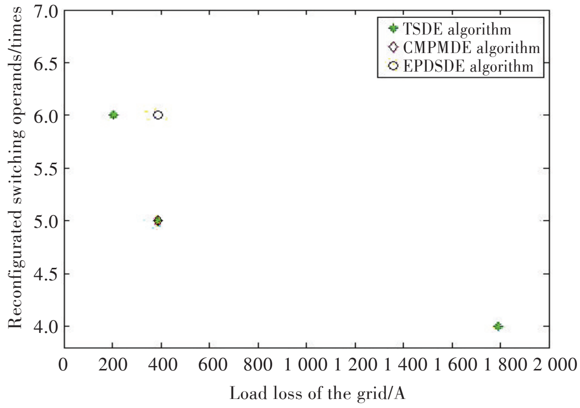

Fig.2 Multi-objective function values of different algorithms under fault 1

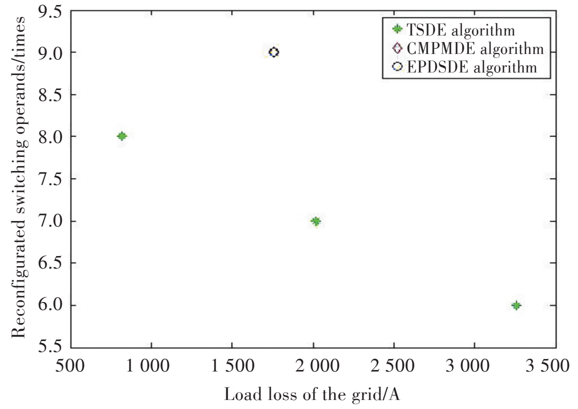

Fig.3 Multi-objective function values of different algorithms under fault 2

In summary, although the convergence speed of the TSDE algorithm is slightly lower than that of the other two algorithms, it has fewer adjustable parameters and better convergence and distribution and is more suitable for practical engineering needs, which can guarantee the safe and stable operation of the ship power system.

5 Conclusions

In order to solve the reconfiguration problem of ship micro-grid, we proposed a constrained multiobjective optimization method based on a two-stage differential evolution algorithm in this paper. In the first stage, the constrained optimization problems are solved by using the two-population hybrid method, and then the first population and the second population after optimization are mixed into one population. This not only allows the adaptive penalty function method and feasibility rule to complement each other but also increases the population diversity, thus improving the convergence and distribution of the optimal non-inferior solution. In the second stage, the improved feasibility rule is adopted to deal with the constrained optimization problem, and an environment Pareto dominated selection strategy is adopted to retain the excellent information of feasible and infeasible solutions. The convergence and distribution of the TSDE algorithm are further improved after the optimization in the second stage. In addition, this paper also introduces the Tent map chaotic sequence, improved non-parametric mutation operator, adaptive crossover factor, and improved elitist selection strategy, which further improves the reconfiguration performance of the differential evolution algorithm.

According to the simulation comparison results under two fault conditions, the non-dominated solution distribution of the TSDE algorithm is more uniform and closer to those of the real Pareto frontier, so this algorithm is more suitable for dealing with the fault reconfiguration problem of ship micro-grid.

References

[1] WANG X H, LI J J, XIAO J M. Greed DPSO algorithm for network reconfiguration of shipboard power system [J]. Control and Decision, 2008, 23 (2): 157-161 (in Chinese).

[2] LI J J, XU B W, GAN S H, et al. Discrete particle swarm optimization algorithm based on greed table for network reconfiguration of the shipboard power system [J]. Transactions of China Electrotechnical Society, 2011, 26(5): 146-151 (in Chinese).

[3] CHEN Y. Shipboard power system fault reconstruction method research based on gaussian dynamic particle swarm optimization algorithm [D]. Dalian: Dalian Maritime University, 2015 (in Chinese).

[4] CHU Y H. Network reconfiguration of shipboard power system based on improved particle swarm optimization algorithm [D]. Zhenjiang: Jiangsu University of Science and Technology, 2016 (in Chinese).

[5] CHU Y H, HUANG Q L. Reconfiguration of shipboard power system based on double sub-swarms particle swarm optimization [J]. Electronic Design Engineering, 2017, 25(5): 37-41 (in Chinese).

[6] DEB K, PRATAP A, AGARWAL S, et al. A fast and elitist multiobjective genetic algorithm: NSGA-II [J]. IEEE Transactions on Evolutionary Computation, 2002, 6(2): 182-197.

[7] YANG X X, ZHANG X F, ZHANG Y, et al. The study of network reconfiguration of the shipboard power system based on heuristic genetic algrithm [J]. Proceedings of the CSEE, 2003, 23(10): 42-46 (in Chinese).

[8] YANG X X, ZHANG X F, ZHANG Y. Study on immune genetic algorithm for shipboard power system service restoration [J]. Proceedings of the CSEE, 2004, 24(9): 80-85 (in Chinese).

[9] ZHANG T. Fault restoration of shipboard power system based on NSGA-II algorithm [D]. Dalian: Dalian Maritime University, 2015 (in Chinese).

[10] ZHU Z Y, LIU W T, ZHUANG X B. Shipboard power system service restoration based on clonal algorithm [J]. Transactions of China Electrotechnical Society, 2009, 24(1): 164-170 (in Chinese).

[11] WANG C J, WANG X H, XIAO J M. Improvement of application of differential evolution algorithm in network reconfiguration of shipboard power system [J]. Ship Engineering, 2013, 35(6): 55-59, 67 (in Chinese).

[12] ZHU Z Y, ZHENG C Y. Network reconfiguration of shipboard power system based on chaos adaptive differential evolution algorithm [J]. Journal of Jiangsu University of Science and Technology (Natural Science Edition), 2013, 27(2): 154-158 (in Chinese).

[13] BI X J, LIU G A. A cloud differential evolutionary algorithm for constrained multi-objective optimization [J]. Journal of Harbin Engineering University, 2012, 33(8): 1022-1031 (in Chinese).

[14] MA L S, ZHANG J D, REN G, et al. Network reconfiguration of ship power system based on chaotic migration and parameterless mutation differential evolution algorithm [J]. Journal of Shanghai Maritime University, 2015, 36(3): 76-81 (in Chinese).

[15] MA L S, ZHANG J D, REN G. Shipboard power grid reconstruction based on environment Pareto dominated selection differential evolution algorithm [J]. Journal of Dalian Maritime University, 2018, 44 (2): 33-38 (in Chinese).

[16] SUN H, YANG J M, LIU X, et al. Differential evolution algorithm based on environment Pareto dominated selection strategy in constrained multi-objective optimization problem [J]. Control and Decision, 2016, 31(1): 45-51 (in Chinese).

基于多目标优化算法的船舶微电网重构

苏丽,王锡淮*,肖健梅
上海海事大学 物流工程学院,上海 201306

摘　要:[**目的**]为了解决现有约束多目标优化算法在求解船舶微电网重构时收敛性和分布性不佳的问题,提出一种基于两阶段差分进化(TSDE)算法的约束多目标优化方法。[**方法**]第1阶段采用双种群混合法(即自适应罚函数法和可行性法则)来处理约束条件;第2阶段将第1阶段产生的双种群合并为单种群,再采用可行性法则解决约束优化问题;最后,在不同的阶段采用不同的精英选择策略和改进无参数变异算子,从而进一步优化差分进化算法。[**结果**]根据算例仿真结果:在故障1和故障2工况下,TSDE算法求得的最小负荷失电量分别比基于混沌迁移及无参数变异差分进化(CMPMDE)算法和基于环境Pareto支配选择差分进化(EPDSDE)算法降低了185 A和940 A;在故障1工况下,TSDE算法的最少开关操作数比CMPMDE算法多1次,与EPDSDE算法相同;在故障2工况下,TSDE算法的最少开关操作数比CMPMDE算法和EPDSDE算法均少1次。[**结论**]TSDE算法求得的最优非劣解集更接近真实的Pareto前沿且分布较为均匀,在满足重构时间要求的前提下,该算法可以更好地保证船舶的安全稳定运行。

关键词:微电网重构;多目标优化;两阶段差分进化算法;精英选择策略;改进无参数变异算子